Published in final edited form as:
Birth Defects Res A Clin Mol Teratol. 2012 October ; 94(10): 804–816. doi:10.1002/bdra.23052.

Bone morphogenetic proteins regulate hinge point formation during neural tube closure by dynamic modulation of apicobasal polarity

Dae Seok Eom[1,#], **Smita Amarnath**[2], **Jennifer L. Fogel**[3,*], and **Seema Agarwala**[1,2,3,‡]

[1]Institute for Cell and Molecular Biology, University of Texas at Austin, TX 78712, USA

[2]Section of Molecular, Cellular and Developmental Biology, University of Texas at Austin, Austin, TX 78713, USA

[3]Institute for Neuroscience, University of Texas at Austin, Austin, TX 78712, USA

Abstract

Background—A critical event in neural tube closure is the formation of median (MHP) and dorsolateral hinge points (DLHP). Together, they buckle the ventral midline, elevate and juxtapose the neural folds for proper neural tube closure. Dynamic cell behaviors occur at hinge points (HPs), but their molecular regulation is largely unexplored. Bone Morphogenetic Proteins (BMPs) have been implicated in a variety of neural tube closure defects, although the underlying mechanisms are poorly understood.

Methods—In this study we used in vivo electroporations, high-resolution microscopy and biochemical analyses to explore the role of BMP signaling in chick midbrain neural tube closure.

Results—We identified a cell-cycle dependent BMP gradient in the midbrain neural plate, which results in low-level BMP activity at the MHP. We show that while BMP signaling does not play a role in midbrain cell-fate specification, its attenuation is necessary and sufficient for MHP formation and midbrain closure. BMP blockade induces MHP formation by regulating apical constriction and basal nuclear migration. Furthermore, BMP signaling is critically important for maintaining epithelial organization by biochemically interacting with apicobasal polarity proteins (e.g., PAR3). Thus prolonged BMP blockade disrupts apical junctions, desegregating the apical (PAR3+, ZO1+) and basolateral (LGL+) compartments. Direct apical LGL-GFP misexpression in turn is sufficient to induce ectopic HPs.

Conclusions—BMPs play a critical role in maintaining epithelial organization, a role that is conserved across species and tissue-types. Its' cell-cycle dependent modulation in the neural plate dynamically regulates apicobasal polarity and helps bend, shape and close the neural tube.

Keywords

Noggin; hinge point; apical constriction; basal nuclear migration; PAR3; Lethal giant larva; tight junctions; adherens junctions; interkinetic nuclear migration; midbrain

‡Author for correspondence (agarwala@mail.utexas.edu).
#Dae Seok Eom's current address: Department of Biology, University of Washington Seattle, WA 98195
*Jennifer Fogel's current address : Stem Cell and Regenerative Medicine; University of Southern California; Los Angeles, CA 90033

Presented at the 7th International Conference on Neural Tube Defects, 2011, Austin, TX.

Introduction

Neural tube closure requires the complex orchestration of cellular events across the folding neural plate. Critical to this process is the formation of the MHP and DLHPs (Colas and Schoenwolf, 2001; Schoenwolf and Smith, 2000; Smith and Schoenwolf, 1997; Ybot-Gonzalez et al., 2002). These serve as pivots around which the neural plate can be bent, shaped and ultimately closed into a neural tube (Smith and Schoenwolf, 1997). Although the relative importance of the MHP and DLHP differs at different axial levels of the neural tube, their absence frequently results in a failure of the neural tube to close (Ybot-Gonzalez et al., 2002; Ybot-Gonzalez et al., 2007).

The formation of HPs entails the dynamic regulation of multiple cell behaviors. These include polarized changes in cell shape (apical constriction), apicobasal length and nuclear location (basal nuclear migration) (Colas and Schoenwolf, 2001). These changes are dynamically modulated over time along the apicobasal and mediolateral axes of the neural plate. While a fair understanding of the cellular events at the HPs has emerged over the last few decades, the molecular bases of how they are dynamically orchestrated in time has so far proved elusive.

The Transforming Growth Factor β (TGFβ) family of signaling molecules, particularly the BMPs, play a critical role in neural induction and dorsal cell fate specification in the neural tube (Liu and Niswander, 2005). Interestingly, a number of mouse lines carrying mutations in TGFβ pathway genes also show severe neural tube closure defects, although the underlying cellular causes of such defects are not understood (Castranio and Mishina, 2009; Chang et al., 1999; McMahon et al., 1998; Solloway and Robertson, 1999; Stottmann et al., 2006; Ybot-Gonzalez et al., 2007).

In recent years, TGFβ family members have been associated with size and shape regulation in diverse tissues such as the gastrulating zebrafish and the *Drosophila* wing (Martin-Castellanos and Edgar, 2002; Teleman et al., 2001; von der Hardt et al., 2007). For example, altered levels of the BMP homolog decapentapleigic (*Dpp*), result in extensive epithelial disruption, apoptosis and a smaller wing size in the fly (Gibson and Perrimon, 2005; Shen and Dahmann, 2005). Interestingly, size reduction in the wing blade due to loss of *Dpp* occurs not as a result of apoptosis as previously supposed, but rather as a result of cytoskeletal disorganization. Such disorganization results in the formation of clusters of cells (cysts or rosettes) which display altered epithelial arrangements and are ultimately expelled from the wing primordium (Gibson and Perrimon, 2005; Shen and Dahmann, 2005). Thus, growth control in the wing by *Dpp* appears to be at least partly due to the ability of TGFβ family members to regulate epithelial organization (Massague, 2008).

A feature of epithelial organization is its apicobasal polarity, marked by the segregation of the apical and basolateral membrane compartments by tight junctions (Margolis and Borg, 2005). This segregation is in part maintained by antagonistic interactions between basolateral proteins (e.g., lethal giant larva, scribble, disks large) and apical, tight junction-associated protein complexes, (e.g., the PAR3-aPKC-PAR6 complex) (Bilder, 2004). *In vitro* studies in mammary gland epithelial cells suggest that TGFβ activation can destabilize tight junctions by phosphorylating PAR6 (Ozdamar et al., 2005). Rho-GTPases are activated as a result, leading to a disruption of tight junctions and epithelial to mesenchymal transitions (EMT, (Ozdamar et al., 2005)). BMPs might also regulate epithelial organization by interacting with cell-adhesion molecules concentrated at adherens junctions. For example, cadherin-mediated BMP activity is essential for the migration of neural crest cells as well as the directional, convergent extension movements that narrow and elongate the fish embryo during gastrulation (Shoval et al., 2007; von der Hardt et al., 2007).

Although the role of BMP signaling in dorsal neural cell-fate specification has been extensively examined, little is known about how this pathway might cause neural tube closure defects in mice with mutations in the TGFβ cascade (Castranio and Mishina, 2009; Liu and Niswander, 2005; Stottmann et al., 2006; Ybot-Gonzalez et al., 2007). To remedy this, we examined the role of BMP signaling in neural tube closure at the midbrain level, a region where exencephaly occurs frequently (Copp et al., 2003). We observed that a complex two-dimensional BMP gradient occurs in the chick midbrain during neurulation, with low level, mosaic, cell-cycle dependent signaling at the MHP. With early *in vivo* manipulations, we show that BMP signaling underlies the dynamic modulation of the epithelial architecture of the midbrain neural plate via regulation of the apicobasal polarity pathway. As a consequence, BMP signaling plays a critical role in the early events involved in neural tube closure.

Materials and Methods

Chick embryos

Fertilized Leghorn eggs (Ideal Poultry, Texas) were incubated at 38°C and the embryos staged according to Hamburger and Hamilton (HH) (Hamburger and Hamilton, 1951).

Expression vectors

In vivo gene expression was driven by the xenopus (pXex), human (pEFX) Elongation-Factor 1∞, pMes or pCS2 promoters (Agarwala et al, 2001; Johnson and Krieg, 1994; Swartz et al., 2001). Embryos were electroporated with EGFP (Agarwala et al., 2001), membrane targeted-EGFP (m-EGFP), Noggin, dominant negative BMP receptors 1A-IRES-EGFP (dnBMPR1A), constitutively active BMP receptor 1A-IRES-EGFP (ca-BMPR1A), BMP4 and EFX-LGL-GFP. EGFP fluorescence was seen within 3 hours of electroporation with Xex and EFX promoters.

In ovo electroporation

Unless mentioned, 0.02–5μg/μl DNA was electroporated into HH stages 4–6 or HH7–11 embryos according to previously established protocols (Agarwala et al., 2001). Electroporated embryos were returned to the incubator for 3 hours–4 days prior to harvesting. Since no differences were noted between phenotypes produced by the early and late electroporations, these data were pooled.

In situ hybridization

Embryos were harvested between HH7-E5 and immersion-fixed in 4% paraformaldehyde. DIG or FL conjugated antisense riboprobes were prepared from cDNAs for *CHORDIN, EGFP, GLI3, NOGGIN, PHOX2A, PAX6, PAX7, SHH* and *WNT1*. One or two color whole-mount in-situ hybridizations were conducted according to previously established protocols (Agarwala and Ragsdale, 2002).

Immunohistochemistry

Embryos were fixed in 4% paraformaldehyde for 15 min–2 hours. Midbrains were sectioned at 14μm in the coronal plane. The following primary antibodies were used for analyses: rabbit anti-pHH3 (Upstate; 1:500), rabbit anti-PAR3 (Upstate; 1:500), rabbit anti-phosphorylated (p)-SMAD 1,5,8 (Cell signaling; 1:1000), mouse anti-N-Cadherin (DSHB; 1:500), mouse anti-ZO-1 (BD biosciences; 1:1000); mouse anti-GFP (Molecular Probes; 1:500), Laminin (DSHB; 1:1000) and activated Caspase 3 (Cell Signaling; 1:200). Alexa-conjugated secondary antibodies were used for fluorescent detection using standard protocols (Afonso and Henrique, 2006). Alexa-conjugated phallotoxins (Molecular Probes)

were used for the direct detection of F- (filamentous) actin. DAPI staining was used for detecting nuclei.

Wholemount pSMAD 1,5,8 immunohistochemistry

Wholemount pSMAD 1,5,8 immunolabeling was conducted according to previously established protocols (Eom et al., 2011).

TUNEL Staining

Wholemount TUNEL staining was conducted in E3 midbrains according to previously established protocols (Agarwala et al., 2005; Yamamoto and Henderson, 1999).

Imaging

Immunofluorescent confocal images were obtained with a Zeiss Laser Scanning Microscope (LSM 5 Pascal) and or with an Olympus IX51 spinning disc microscope (Olympus) and captured with AxioVision (Zeiss) or Slide Book Pro software. Data analyses were conducted using Imaris (Bitplane), Adobe Photoshop and Adobe Illustrator. Unless mentioned, confocal images are presented as single 0.5–0.8 μm thick optical sections.

Immunoprecipitation and western blot analysis

For Western Blot analyses, whole cell lysates were prepared from HH9–11 wild-type midbrains or the electroporated regions of E3 midbrains. We first confirmed that HPs induced at HH7-E5 by Noggin-electroporations at HH4–11 were identical in every way to the endogenous MHP based on morphological, cellular and molecular criteria. This permitted us to collect lysates from wild-type brains and electroporated brains between HH9-E3. Tissue lysates were prepared as previously described (Eom et al., 2011). 100μg of protein from chick midbrains was incubated with either 10 μg/ml of normal rabbit IgG (Alpha Diagnostic Intl. Inc) or 20 μg/ml of anti-PAR3 (Millipore), or anti-pSMAD 1,5,8 (Cell Signaling). Protein complexes were immunoprecipitated using 20μl of protein A/G agarose beads, separated by SDS-PAGE, immunoblotted with PAR3 or pSMAD 1/5/8 antibodies and detected by ECL chemiluminescence (Thermoscientific; IL). The molecular weight of the PAR3 and pSMAD 1,5,8 was ascertained using NCBI databases.

Quantitative Analyses

All quantification in this study was conducted using ImageJ software (NIH) on midbrains electroporated at HH4–11 and harvested at HH7-E3. Unless mentioned, quantitative data was obtained from 2–3 (14μm) sections/per control or Noggin-electroporated brain at the rostrocaudal midpoint of the midbrain. Data was displayed as the mean ± s.e.m. Statistical significance was evaluated using an unpaired Student's *t*-test.

pSMAD 1,5,8 cell distribution in the neural plate—HH7 midbrain wholemounts (n=5) were flattened and a measure of the latero-medial gradient was obtained by counting all apically visible pSMAD 1,5,8+ cells in the MHP and lateral neural plate. The numbers of MHP and lateral neural plate cells were compared using a *t*-test.

Apical Constriction—A direct measurement of apical constriction was made in mEGFP and Noggin+mEGFP electroporated flattened wholemounts stained with PAR3. Since the effects of Noggin and dnBMPR1 were non-autonomous, a sampling box subtending 50μm × 50μm was drawn in ventrolateral midbrain and the apical surface areas of all cells or only electroporated cells within the sampling box were measured using ImageJ (Control: n=48cells/3brains; Noggin-electroporated brains: Noggin+ cells: n=161cells/4brains; All cells: n=435cells/3brains). Pairwise comparisons between control and Noggin-

electroporated cells and control and all cells within the sampling box were made using a *t*-test.

Basal Nuclear Migration—The distance of mitotic (pHH3+) cells from the apical surface was determined by drawing a straight line from the apical surface to the apical tip of each pHH3+ cell in control (n=3 embryos; 271 cells) and Noggin electroporated embryos (n=5 embryos; 313 cells). The differences were evaluated using a *t*-test. Basal nuclear migration for all cells was also determined by centering a 70μm ×70μm sampling box in control lateral neural plate or at ectopic HPs induced by Noggin electroporations in lateral neural plate. A perpendicular line was drawn from the PAR3+ apical surface to the apical tip of each DAPI+ nucleus in the sampling box. Differences were evaluated using a *t* test.

Apicobasal Length—The apicobasal span of midbrain progenitors was measured in early HH7 brains electroporated with mEGFP alone or in conjunction with Noggin. A sampling box was positioned in ventrolateral midbrain as above. Within the box, the apicobasal spans of all electroporated cells whose outline could be fully visualized in control (n=17 cells/5 brains) and Noggin-electroporated midbrains (n=42 cells/10 brains) were measured and compared using a *t*-test.

Results

A 2-dimensional, spatiotemporally dynamic BMP gradient in the neural plate

We examined BMP signaling in the neurulating chick embryo between HH Stages 4–10 (Colas and Schoenwolf, 2001; Hamburger and Hamilton, 1951). BMP ligands as well as BMP antagonists (*Chordin* and *Noggin*) were expressed in the MHP and the notochord of the folding neural plate in complex patterns (Fig. 1A, B; data not shown). The high levels of Chordin and Noggin at the axial midline of the neural plate coincided with low levels of pSMAD 1,5,8, a definitive readout of canonical BMP signaling (Fig. 1C–H). Interestingly, pSMAD 1,5,8 expression formed a complex two-dimensional spatio-temporal gradient in the neural plate (Fig. 1C–H). A mosaic, lateral to medial, gradient of pSMAD 1/5/8 spanned the neural plate, with high numbers of pSMAD 1,5,8 cells in lateral neural plate and low numbers at the MHP {84.4 cells (lateral neural plate) vs.12 cells (MHP); $p=3.84\times10^{-6}$; Fig. 1C, inset C; 1D, G, H}. In the neurectoderm, nuclei execute interkinetic nuclear migration along the apicobasal/ventricular pial axis, invariably undergoing mitosis at the apical surface (Sauer, 1935; Smith and Schoenwolf, 1997). We noted that 100% of pHH3+ mitotic cells exhibited high levels of pSMAD 1,5,8 expression apically (Fig. 1E–H; inset H). pSMAD 1,5,8 expression was turned down as nuclei progressed through other phases of the cell cycle (Fig. 1E–H). Since cell cycle duration at the MHP is considerably longer than that in lateral neural plate, fewer pHH3+/pSMAD 1,5,8+ mitotic cells were seen in the MHP than at any other place in the neural plate (Fig. 1C–H; arrowhead in 1H (Smith and Schoenwolf, 1987)). Taken together, these data suggest that low level, mosaic, cell-cycle dependent pSmad 1,5,8 expression occurs at the MHP during neural tube closure.

BMP signaling regulates midbrain morphogenesis, but not ventral cell fate specification

To examine the role of BMP signaling, we misexpressed constitutively active BMP receptor 1A (caBMPR1A), Noggin and dominant negative BMP receptor 1A (dnBMPR1A) in the ventral midbrain using in ovo electroporation. Noggin overexpression between HH4–11 resulted in lowered pSMAD 1,5,8 expression, suggesting that canonical BMP signaling was reduced in the midbrain (Fig. 2A, B). Despite significant pSMAD1,5,8 reduction, *SHH* (floor plate), *PHOX2A* (oculomotor neurons) and *PAX6* expression suggested that ventral cell-fates were correctly specified in the midbrain (Fig 2C, D). Increased BMP signaling by caBMPR1 or BMP4 misexpression similarly did not affect ventral midbrain fate

specification (Fig. 2E, F; data not shown). By contrast, Noggin-electroporated midbrains displayed dramatically altered shapes, suggesting a role for BMP signal attenuation in midbrain morphogenesis (Fig. 2G, H). Of particular interest to us were the ectopic hinge-like invaginations of the apical surface (arrowheads Fig. 2H) and the ectopic clusters of neurons (arrow, Fig. 2H) in the lumen of Noggin-electroporated midbrains.

BMP signal modulation is necessary and sufficient for MHP formation

Previous studies have proposed a role for BMP attenuation in DLHP induction in the spinal cord (Stottman et al., 2006; Ybot-Gonzales et al., 2007). Given the expression of BMP antagonists (Noggin, Chordin) in the MHP and the notochord, and the ability of Noggin to elicit hinge-like invaginations, we asked whether BMP blockade might also play a role in MHP formation in the midbrain (Fig. 1A, B; 2F).

Noggin misexpression between HH4–11 dramatically exaggerated the endogenous MHP (n=18/23; Fig. 3A, A′; B, B′). By contrast, increased BMP signaling by caBMPR1 misexpression resulted in a dramatic flattening of the MHP (n=15/24; Fig. 3C, C′). Thus, although BMP blockade did not induce ventral midline cell-fates, it was both necessary and sufficient for endogenous MHP formation in the midbrain (Fig. 2C–F; Fig. 3A–C′). Together with previously published studies, these data suggest that BMP blockade underlies both MHP and DLHP formation in the neural tube (Eom et al., 2011; Ybot-Gonzales et al., 2007).

The results above indicated that BMP blockade between HH4–11 produced HP formation at E2–E5 (Fig. 2H; 3A, B). We next asked whether BMP blockade would induce MHP formation during the endogenous phase of MHP formation (HH4–8) and whether the effects would be cell-autonomous. We therefore switched to HH4–6 electroporations of dnBMPR1 misexpression and examined the midbrain at HH7 when MHP formation is ongoing (Brown et al., 2012a, b; Eom et al., 2011). As with Noggin, dnBMPR1 misexpression was sufficient to deepen the endogenous MHP, and to induce ectopic HPs in lateral neural plate at HH7 (Fig. 3D–G). These results also demonstrated that both electroporated and un-electroporated cells participated in ectopic HP formation, suggesting that the effects of BMP blockade were at least partially non-autonomous (Fig. 3E, G; 5D″; 7B; 7F).

Interestingly, both BMP gain and loss of function manipulations, which altered the contours of the MHP, also prevented the neural folds from drawing together and closing correctly (n=8/12, arrowheads, Fig. 3H–J). Together, these results suggest that BMP signal attenuation is both necessary and sufficient for MHP formation. Furthermore, they show that unlike caudal spinal cord, MHP formation is required for neural tube closure at the midbrain level (Ybot-Gonzalez et al., 2007).

BMP signaling does not affect dorsal midbrain cell fates

BMP signaling plays a role in cell fate specification in the dorsal spinal cord (Liu and Niswander, 2005). By contrast, studies from other laboratories showed that manipulations of BMPR1B receptors do not alter avian dorsal midbrain cell fates (Bobak et al., 2009). However, given the large number of BMP type I and II receptors, it was still possible that the midbrain closure defects shown in Fig. 3 were an indirect consequence of BMPR1B-independent, BMP-dependent changes in dorsal cell-fates. To address this issue, we misexpressed Noggin, BMP4 and caBMPR1 in dorsal midbrain. Unlike the morphogenetic effects at the MHP, which could be induced at low levels (≥0.2μg/μl) of Noggin misexpression, high levels (≥ 3 μg/μl) of BMP manipulations were required to elicit effects on dorsal midbrain cell fates (Fig. 4A–F; data not shown). Such BMP gain and loss of function experiments suggested a role for BMP signaling in *WNT1* induction in the roof

plate (Fig 4A–F). Importantly, BMP-induced changes in *WNT1* expression did not interfere with the ability of the dorsal midline to fuse (Fig. 4A–F), most likely because roof plate induction occurs ~ HH10 in the midbrain, well after dorsal midline fusion at HH8. Besides its specific role in roof plate induction, even high levels (3–5 μg/μl) of dorsal BMP blockade or misexpression did not reliably affect overall dorsal midbrain patterning, as shown by the normal expression patterns of *GLI3* and *PAX7* (Fig. 4A–F). Together with the results shown in Fig. 2C–F, we concluded that BMP signaling does not play a significant role in either dorsal or ventral midbrain cell fate specification. Interestingly, targeted dorsal BMP manipulations did not affect the contours of the ventral midline, suggesting that the morphogenetic effects of BMP signaling at the ventral midline were not a secondary consequence of altered cell fates, either dorsal or ventral.

BMP blockade regulates the dynamic cell behaviors required to form the MHP

We next explored the role of BMP signaling on cell behaviors (apical constriction and the basal migration of nuclei) that are essential for the formation of HPs in the neural plate (Colas and Schoenwolf, 2001; Smith and Schoenwolf, 1997) (Fig. 5A). To visualize the apical surface of cells, we electroporated midbrains with either membrane-targeted EGFP (m-EGFP) alone or in conjunction with Noggin. Midbrain wholemounts stained with the apical marker PAR3 were flattened to visualize the apical surface of electroporated cells (see cartoon in Fig. 5B). Severe cell-autonomous and non-autonomous apical constriction was seen in Noggin-electroporated cells whose apical surface areas were 68% smaller than cells in control brains (Fig. 5C–E; apical surface area: control cells: 25.79μm^2; Noggin-electroporated cells: 8.35μm^2; $p=5.67\times10^{-21}$). Similar results were obtained when control apical surface areas were compared with all cells within the sampling box as described in the Materials and Methods (Fig. 5E; control cells: 25.79μm^2; all cells: 8.5μm^2; $p=3.99\times10^{-14}$). Thus, BMP attenuation was sufficient to induce apical constriction in the neural plate.

One mechanism to obtain the reduced apical cell-surface areas seen at the endogenous MHP is to move nuclei away from the apical surface of the neurectoderm, a phenomenon termed basal nuclear migration (Colas and Schoenwolf, 2001). To determine whether BMP blockade induces basal nuclear migration, we examined the apicobasal location of Noggin-electroporated mitotic (pHH3+) nuclei, which occur within 2 nuclear depths of the apical surface in wild-type brains ((Smith and Schoenwolf, 1987); Fig. 5F). Within 6 hours of Noggin electroporations, we noted that increased numbers of pHH3+ mitotic nuclei were located more basally, relative to control brains (distance from the apical surface, control: 5.2μm; Noggin: 15.32μm; $p=2.32\times10^{-19}$; Fig. 5F, G, J). To confirm these results for all affected nuclei, we next examined the apicobasal location of DAPI-stained nuclei in control and Noggin-electroporated brains. Compared to EGFP-electroporated controls, nuclei at Noggin-induced HPs were also more basally located (Fig. 5H–I′; K; distance from the apical surface, control: 8.15μm; Noggin: 18.14μm; $p=3.15\times10^{-7}$). Thus, BMP blockade can induce apical constriction and the basal migration of nuclei associated with HP formation.

The apicobasal length of MHP cells is shorter than that of lateral neural plate cells (Fig. 5A). However, Noggin-electroporated cells increased their apicobasal length by 30% within 6 hours of electroporation (Fig. 5L; Fig. 6D, E). Thus while BMP blockade can induce apical constriction and basal nuclear migration, it is not sufficient to induce apicobasal shortening. However, the increased apicobasal length does not preclude the formation of ectopic HPs in lateral neural plate in response to Noggin misexpression.

BMPs regulate apicobasal polarity pathway genes

The data above show that BMP signaling regulates cell behaviors along the apicobasal axis in developing midbrain. We therefore asked if BMP signaling might regulate the apicobasal

polarity pathway in the developing neural tube. In control brains, proteins associated with tight (PAR3, ZO1) junctions were seen along the apical surface of the midbrain neurectoderm (Fig. 6A, A′; data not shown). Strikingly, Noggin electroporations resulted in the downregulation of PAR3 and ZO1 from the apical compartment (Fig. 6A–6B′, data not shown). These effects were partially rescued by co-electroporations of BMP4 and Noggin (Fig. 6C, C′; data not shown).

Previous work has shown that PAR3 and LGL can compete for association with the PAR6-aPKC polarity complex at the tight junction (Plant et al., 2003; Yamanaka et al., 2003). To determine whether the Noggin-induced downregulation of PAR3 from the apical compartment resulted in a concomitant increase in apical LGL, we visualized the apical and basolateral compartments simultaneously by combining low-level (1μg/μl) electroporations of LGL-GFP fusion protein with PAR3 immunolabeling (Dollar et al., 2005). A clear segregation between the basolateral (LGL+) and the apical (PAR3+) compartments demonstrated that these levels of LGL-GFP did not affect neural apicobasal polarity (Fig. 6D-D″). However, when LGL-GFP and Noggin (1μg/μl each) were co-electroporated, ectopic LGL could be seen along the apical surface where PAR3 is normally expressed (Fig. 6E-E″). Together, these data suggest that BMP blockade alters apicobasal polarity.

We next conducted Western Blot analyses to determine whether BMP blockade reduced PAR3 protein levels. These analyses demonstrated that BMP blockade did not reduce total PAR3 protein levels, but altered its subcellular localization (Fig. 6F). We noted that unlike controls, Noggin-electroporated midbrains displayed PAR3+ puncta in the cytoplasm (Fig. 6A–C′; arrows, Fig 6B′, C′). These results were confirmed by the mislocalization of the adherens junction protein N-CAD into the cytoplasm following BMP blockade (arrowheads and arrows, Fig. 6H, H′). Taken together, these results suggest that BMP signaling regulates the integrity of epithelial organization by controlling the subcellular localization of apicobasal polarity pathway proteins.

Perturbations of the apicobasal polarity pathway are sufficient to induce HP formation

Overexpression of Noggin results in the ectopic apical localization of LGL (Fig. 6E-E″). We reasoned that if BMP attenuation regulates HP formation via the apicobasal polarity pathway, then direct apical misexpression of LGL might mimic the effects of BMP blockade. Unlike low-levels of LGL-GFP misexpression, which did not affect polarity (Fig. 6D), high-levels (5ug/ul) of LGL-GFP misexpression replicated multiple phenotypes seen with Noggin overexpression. These included the induction of ectopic hinge points (Fig. 7A, B), apically constriction (Fig. 7C, D), basal nuclear migration (Fig. 7A, E), and subapical mitosis (Fig. 7F, G). We conclude that BMP blockade results in ectopic apical LGL mislocalization. Apical LGL expression in turn is sufficient to account for much of the epithelial dysmorphology seen following BMP blockade.

BMP pathway members biochemically interact with apical junctional proteins

We next asked whether the BMP signaling cascade biochemically interacted with members of the apicobasal polarity pathway. Strikingly, immunoprecipitation of HH 9–11 brain lysates with pSMAD 1,5,8 antibody (specific for the phosphorylated forms of SMAD1,5,8) followed by immunoblotting with PAR3 or vice versa, demonstrated a biochemical interaction between the effectors of canonical BMP signaling and the apicobasal polarity pathway (Fig. 7H, H′). These interactions were attenuated by Noggin electroporations (Fig. 7I, I′).

The epithelial dysmorphology resulting from BMP blockade is consistent with dysregulation of the apicobasal polarity pathway

Disruptions of epithelial organization result in a heterogeneous set of phenotypes that can ultimately lead to EMT and cell delamination (Bryant and Mostov, 2008). We therefore asked whether sustained BMP blockade might produce other phenotypes associated with the loss of apicobasal cell polarity (Ozdamar et al., 2005). Phalloidin staining demonstrated that the epithelial organization and cell-shapes in the midbrain neurectoderm were severely compromised in Noggin-electroporated brains (Fig. 8A, B). Activated caspase 3 and TUNEL staining suggested that while cell death was increased in Noggin-electroporated embryos, the changes in cell shape and epithelial organization could occur independent of cell death (Fig. 8C–F).

In extreme cases, the disrupted epithelial organization resulted in a full EMT with neurons delaminating into the lumen of neural tube (Fig. 8E, F; Supplementary Fig. 3A, B). The absence of PAR3 and the presence of apical processes in the lumen of the neural tube further corroborated the EMT phenotype (Supplementary Fig. S3A, B). Previous studies have shown that epithelial remodeling results in a special type of apoptosis (anoikis), which results from a failure of epithelial cells to remain associated with their neighbors or the extracellular matrix (Gilmore, 2005; Massa et al., 2009). Indeed TUNEL staining following Noggin misexpression revealed that the delaminated cells were frequently removed from the lumen of the neural tube by apoptosis (Fig. 8E, F).

Three-dimensional tissue culture experiments suggest that the dynamic modulation of polarity can produce heterogeneous phenotypes and complex tissue arrangements, such as cysts or simple or branched tubules (Bryant and Mostov, 2008; Martin-Belmonte et al., 2008). Consistent with this idea, Noggin-electroporated midbrains frequently displayed cells that had organized themselves into cysts (Fig. 8E–H). Such cysts displayed a PAR3+ ZO1+, pHH3+ apical surface surrounding a central lumen and typically contained just a small number of electroporated cells (Fig. 8G, H; Supplementary Fig. S3C–D′). Furthermore, they behaved like *dpp*$^{-}$ cell clones in the fly wing and frequently migrated out of the neural tube into neighboring tissues (Fig. 8G; Supplementary Fig. S3D, D′). (Gibson and Perrimon, 2005; Shen and Dahmann, 2005). We also noted that Noggin electroporations resulted in a disrupted Laminin+ basal lamina, suggesting the latter as a mechanism for cyst migration (Fig. 8I, J)

We noted that unlike normal midbrain progenitors which displayed few filopodia-like-processes, Noggin-electroporated cells displayed abundant lateral filopodia (arrowheads, (Fig. 8K–L′). Such filopodial structures might provide the cellular basis for the increased ability of Noggin-induced cysts to migrate out of the neural tube into adjacent tissues. Since increased cell motility is a hallmark of EMT (e.g. during cancer metastasis), these data provide further evidence for the interactions between BMP signaling and the regulation of apicobasal polarity.

Discussion

In this study, we provide evidence for a role for BMP signaling in MHP formation via the regulation of polarity proteins (summarized in Fig. 9). We show that BMP blockade reduces the apical levels of tight junction proteins (e.g., PAR3, ZO1) and increases the apical levels of basolateral proteins (e.g., LGL). Apical LGL misexpression in turn can mimic the effects of BMP blockade and induce ectopic HP formation in the midbrain. BMP and polarity modulation also converge on other cellular phenotypes including altered cell shape, basal nuclear migration and aberrant, sub-apical mitosis. Most significantly, biochemical experiments suggest that pSMAD 1,5,8 and polarity proteins (e.g., PAR3) physically

associated with each other. We conclude that a major function of BMP signaling is the regulation of the apicobasal polarity pathway, a specific consequence of which is the regulation of MHP formation in the neurulating midbrain.

The non-autonomy of BMP function during MHP formation

Only a small number of cells at the neurulating ventral midline at any given time are pSMAD 1,5,8+. How do such few cells bring about a complex, non-autonomous event like HP formation? While the answer to this is not known, we noted that a few cells electroporated with Noggin, dnBMPR1A, or LGL-GFP are sufficient to induce changes in cell behaviors in the electroporated cells and their neighbors. These cell behaviors include HP formation, apical constriction, basal nuclear migration, epithelial disorganization or rosette formation. Similar non-autonomous effects have been noted in the fly embryo where cells with altered polarity can direct the polarity of their neighbors in a non-autonomous fashion (Zallen and Wieschaus, 2004). One possibility is that the non-autonomous effects are communicated across cells via the adherens belt, which is clearly affected by BMP manipulations. Alternatively, the non-autonomy could be a consequence of the mechanical constraints imposed by being associated with neighboring cells either via apical junctions or via the basal lamina.

Dynamic Modulation of Polarity by BMP Signaling

In this study, we show that pSMAD 1,5,8 biochemically interacts with PAR3, an apical protein associated with the tight junction and required for the segregation between apical and basal membrane compartments (Margolis and Borg, 2005). In previous work, we have shown that pSMAD 1,5,8 also interacts with PAR6 and aPKC, two other members of the PAR polarity complex (Eom et al., 2011). Previous work has shown that the PAR complex is associated with the tight junction and responsible for conferring apical membranes their identity (Macara, 2004). Thus, we tentatively place pSMAD 1,5,8 proteins at the tight junction. Analyses of BMP signal transduction suggest that Noggin prevents the ligand-dependent phosphorylation of SMAD 1,5,8 proteins and reduces pSMAD 1,5,8-PAR3 interactions without reducing the levels of PAR3 or absolute levels of SMAD proteins (Eom et al., 2011; Massague et al., 2005). Thus the interactions between pSMAD 1,5,8 and the PAR complex are likely to be ligand-dependent, placing phosphorylated SMAD proteins at the tight junction under conditions of BMP stimulation.

Our data suggest that the ligand-dependent association between the PAR complex and pSMAD 1,5,8 stabilizes the tight junctions and maintains epithelial integrity. In the absence of BMP signaling, the junctions are compromised and LGL can cross into the apical compartment. Simultaneously, PAR3, ZO1 and N-CAD are moved into the cytoplasm. Our previous data suggest that the removal of apical membranes and proteins into the cytoplasm is likely to depend upon endocytosis (Eom et al., 2011). Endocytosis-dependent internalization of apical membranes may therefore be a partial cause of BMP blockade-dependent apical constriction. Similar endocytosis dependent apical constriction has also been reported in bottle cells during frog gastrulation (Lee and Harland, 2010).

Since the BMP signal in the neural plate is cell cycle dependent, we speculate that cells transition between being fully epithelial to partially epithelial over the course of a cell cycle. Since cell cycle progression in the neurectoderm is asynchronous, this means that a partially polarized cell is likely to be flanked by neighbors that are fully or partially polarized. Recent studies have also shown that an initially unpolarized cell can transform itself into a complex structure such as a cyst and then a branched tubule over time by simultaneously dividing and alternating between unpolarized, semipolarized and polarized states, each influenced by distinct sets of signals (Mostov et al., 2003).

Neural progenitors that are cyclically responsive to BMP signaling could similarly alternate between different polarized states as they progress through the cell cycle along the apicobasal axis (Bayly et al., 2007; Eom et al., 2011). The resulting modulations in polarity would provide cells with the flexibility to change their shapes in a dynamic manner and help shape the neural plate. However, each cell would return to a fully polarized state over the course of a single cell cycle, ensuring that it does not undergo a full-scale EMT. This dynamic modulation of polarity, together with the asynchronous nature of cell cycle progression, would in turn ensure that the neuroepithelium retains its overall epithelial organization, while allowing modulations in cell shape. The mediolateral BMP activity gradient would provide a mechanism by which modulations in polarity could be targeted in a regional manner (e.g., MHP), so that shape changes could be orchestrated throughout the neural plate and the neural plate could be bent and shaped as a whole into a neural tube.

Supplementary Material

Refer to Web version on PubMed Central for supplementary material.

Acknowledgments

We thank Drs. Y. Wakamatsu, C. Ragsdale, L. Niswander, D. Duprez, S. Sokol and M. Takeichi, B. Houston, P. Brickell, D. Wu, C. Tabin, A. Graham, J. Cooke, C. Goridis, M. Goulding, G. Martin, A. McMahon and A. Ruegels for reagents. We also would like to thank J. Gross for use of his confocal microscope. This work was supported by an NIH-NINDS grant to SA.

Funding: NIH/NINDS: R01 NS049091

Abbreviations

BMPR1	BMP receptor 1A
ca	constitutively active
dn	dominant negative
EP	electroporation
FP	floor plate
HH	Hamburger and Hamilton stages
L	lumen
MHB	midbrain-hindbrain boundary
MHP	median hinge point
MB	midbrain
NC	notochord
NF	neural fold
NP	neural plate
OMC	oculomotor complex
PHAL	Phalloidin, RP, roof plate

References

Afonso C, Henrique D. PAR3 acts as a molecular organizer to define the apical domain of chick neuroepithelial cells. J Cell Sci. 2006; 119(Pt 20):4293–4304. [PubMed: 17003110]

Agarwala S, Aglyamova GV, Marma AK, Fallon JF, Ragsdale CW. Differential susceptibility of midbrain and spinal cord patterning to floor plate defects in the talpid2 mutant. Dev Biol. 2005; 288(1):206–220. [PubMed: 16246323]

Agarwala S, Ragsdale CW. A role for midbrain arcs in nucleogenesis. Development. 2002; 129(24): 5779–5788. [PubMed: 12421716]

Agarwala S, Sanders TA, Ragsdale CW. Sonic hedgehog control of size and shape in midbrain pattern formation. Science. 2001; 291(5511):2147–2150. [PubMed: 11251119]

Bayly RD, Ngo M, Aglyamova GV, Agarwala S. Regulation of ventral midbrain patterning by Hedgehog signaling. Development. 2007; 134(11):2115–2124. [PubMed: 17507412]

Bilder D. Epithelial polarity and proliferation control: links from the Drosophila neoplastic tumor suppressors. Genes Dev. 2004; 18(16):1909–25. [PubMed: 15314019]

Bobak N, Agoston Z, Schulte D. Evidence against involvement of Bmp receptor 1b signaling in fate specification of the chick mesencephalic alar plate at HH16. Neurosci Lett. 2009; 461(3):223–8. [PubMed: 19539011]

Brown CY, Eom DS, Amarnath S, Agarwala S. A simple technique for early in vivo electroporation of E1 chick embryos. Dev Dyn. 2012; 241(3):545. [PubMed: 22274994]

Bryant DM, Mostov KE. From cells to organs: building polarized tissue. Nat Rev Mol Cell Biol. 2008; 9(11):887–901. [PubMed: 18946477]

Castranio T, Mishina Y. Bmp2 is required for cephalic neural tube closure in the mouse. Dev Dyn. 2009; 238(1):110–122. [PubMed: 19097048]

Chang H, Huylebroeck D, Verschueren K, Guo Q, Matzuk MM, Zwijsen A. Smad5 knockout mice die at mid-gestation due to multiple embryonic and extraembryonic defects. Development. 1999; 126(8):1631–1642. [PubMed: 10079226]

Colas JF, Schoenwolf GC. Towards a cellular and molecular understanding of neurulation. Dev Dyn. 2001; 221(2):117–145. [PubMed: 11376482]

Copp AJ, Greene ND, Murdoch JN. The genetic basis of mammalian neurulation. Nat Rev Genet. 2003; 4(10):784–793. [PubMed: 13679871]

Dollar GL, Weber U, Mlodzik M, Sokol SY. Regulation of Lethal giant larvae by Dishevelled. Nature. 2005; 437(7063):1376–1380. [PubMed: 16251968]

Eom DS, Amarnath S, Fogel JL, Agarwala S. Bone morphogenetic proteins regulate neural tube closure by interacting with the apicobasal polarity pathway. Development. 2011; 138(15):3179–3188. [PubMed: 21750029]

Gibson MC, Perrimon N. Extrusion and death of DPP/BMP-compromised epithelial cells in the developing Drosophila wing. Science. 2005; 307(5716):1785–1789. [PubMed: 15774762]

Gilmore AP. Anoikis. Cell Death Differ. 2005; 12(Suppl 2):1473–1477. [PubMed: 16247493]

Hamburger V, Hamilton HL. A series of normal stages in the development of the chick embryo. J Morph. 1951; 88:49.

Johnson AD, Krieg PA. pXeX, a vector for efficient expression of cloned sequences in Xenopus embryos. Gene. 1994; 147(2):223–226. [PubMed: 7926804]

Lee JY, Harland RM. Endocytosis is required for efficient apical constriction during Xenopus gastrulation. Curr Biol. 2010; 20(3):253–258. [PubMed: 20096583]

Liu A, Niswander LA. Bone morphogenetic protein signalling and vertebrate nervous system development. Nat Rev Neurosci. 2005; 6(12):945–954. [PubMed: 16340955]

Macara IG. Par proteins: partners in polarization. Curr Biol. 2004; 14(4):R160–162. [PubMed: 15027470]

Margolis B, Borg JP. Apicobasal polarity complexes. J Cell Sci. 2005; 118(Pt 22):5157–5159. [PubMed: 16280548]

Martin-Belmonte F, Yu W, Rodriguez-Fraticelli AE, Ewald AJ, Werb Z, Alonso MA, Mostov K. Cell-polarity dynamics controls the mechanism of lumen formation in epithelial morphogenesis. Curr Biol. 2008; 18(7):507–513. [PubMed: 18394894]

Martin-Castellanos C, Edgar BA. A characterization of the effects of Dpp signaling on cell growth and proliferation in the Drosophila wing. Development. 2002; 129(4):1003–1013. [PubMed: 11861483]

Massa V, Greene ND, Copp AJ. Do cells become homeless during neural tube closure? Cell Cycle. 2009; 8(16):2479–2480. [PubMed: 19657232]

Massague J. TGFbeta in Cancer. Cell. 2008; 134(2):215–230. [PubMed: 18662538]

Massague J, Seoane J, Wotton D. Smad transcription factors. Genes Dev. 2005; 19(23):2783–2810. [PubMed: 16322555]

McMahon JA, Takada S, Zimmerman LB, Fan CM, Harland RM, McMahon AP. Noggin-mediated antagonism of BMP signaling is required for growth and patterning of the neural tube and somite. Genes Dev. 1998; 12(10):1438–1452. [PubMed: 9585504]

Mostov K, Su T, ter Beest M. Polarized epithelial membrane traffic: conservation and plasticity. Nat Cell Biol. 2003; 5(4):287–293. [PubMed: 12669082]

Ozdamar B, Bose R, Barrios-Rodiles M, Wang HR, Zhang Y, Wrana JL. Regulation of the polarity protein Par6 by TGFbeta receptors controls epithelial cell plasticity. Science. 2005; 307(5715): 1603–1609. [PubMed: 15761148]

Plant PJ, Fawcett JP, Lin DC, Holdorf AD, Binns K, Kulkarni S, Pawson T. A polarity complex of mPar-6 and atypical PKC binds, phosphorylates and regulates mammalian Lgl. Nat Cell Biol. 2003; 5(4):301–308. [PubMed: 12629547]

Sauer L. Mitosis in the neural tube. J Comp Neurol. 1935; 62(62):377–397.

Schoenwolf GC, Smith JL. Mechanisms of neurulation. Methods Mol Biol. 2000; 136:125–134. [PubMed: 10840705]

Shen J, Dahmann C. Extrusion of cells with inappropriate Dpp signaling from Drosophila wing disc epithelia. Science. 2005; 307(5716):1789–1790. [PubMed: 15774763]

Shoval I, Ludwig A, Kalcheim C. Antagonistic roles of full-length N-cadherin and its soluble BMP cleavage product in neural crest delamination. Development. 2007; 134(3):491–501. [PubMed: 17185320]

Smith JL, Schoenwolf GC. Cell cycle and neuroepithelial cell shape during bending of the chick neural plate. Anat Rec. 1987; 218(2):196–206. [PubMed: 3619087]

Smith JL, Schoenwolf GC. Neurulation: coming to closure. Trends Neurosci. 1997; 20(11):510–517. [PubMed: 9364665]

Solloway MJ, Robertson EJ. Early embryonic lethality in Bmp5; Bmp7 double mutant mice suggests functional redundancy within the 60A subgroup. Development. 1999; 126(8):1753–1768. [PubMed: 10079236]

Stottmann RW, Berrong M, Matta K, Choi M, Klingensmith J. The BMP antagonist Noggin promotes cranial and spinal neurulation by distinct mechanisms. Dev Biol. 2006; 295(2):647–663. [PubMed: 16712836]

Swartz M, Eberhart J, Mastick GS, Krull CE. Sparking new frontiers: using in vivo electroporation for genetic manipulations. Dev Biol. 2001; 233(1):13–21. [PubMed: 11319854]

Teleman AA, Strigini M, Cohen SM. Shaping morphogen gradients. Cell. 2001; 105(5):559–562. [PubMed: 11389824]

von der Hardt S, Bakkers J, Inbal A, Carvalho L, Solnica-Krezel L, Heisenberg CP, Hammerschmidt M. The Bmp gradient of the zebrafish gastrula guides migrating lateral cells by regulating cell-cell adhesion. Curr Biol. 2007; 17(6):475–487. [PubMed: 17331724]

Yamamoto Y, Henderson CE. Patterns of programmed cell death in populations of developing spinal motoneurons in chicken, mouse, and rat. Dev Biol. 1999; 214(1):60–71. [PubMed: 10491257]

Yamanaka T, Horikoshi Y, Sugiyama Y, Ishiyama C, Suzuki A, Hirose T, Iwamatsu A, Shinohara A, Ohno S. Mammalian Lgl forms a protein complex with PAR-6 and aPKC independently of PAR-3 to regulate epithelial cell polarity. Curr Biol. 2003; 13(9):734–43. [PubMed: 12725730]

Ybot-Gonzalez P, Cogram P, Gerrelli D, Copp AJ. Sonic hedgehog and the molecular regulation of mouse neural tube closure. Development. 2002; 129(10):2507–2517. [PubMed: 11973281]

Ybot-Gonzalez P, Gaston-Massuet C, Girdler G, Klingensmith J, Arkell R, Greene ND, Copp AJ. Neural plate morphogenesis during mouse neurulation is regulated by antagonism of Bmp signalling. Development. 2007; 134(17):3203–3211. [PubMed: 17693602]

Zallen JA, Wieschaus E. Patterned gene expression directs bipolar planar polarity in Drosophila. Dev Cell. 2004; 6(3):343–355. [PubMed: 15030758]

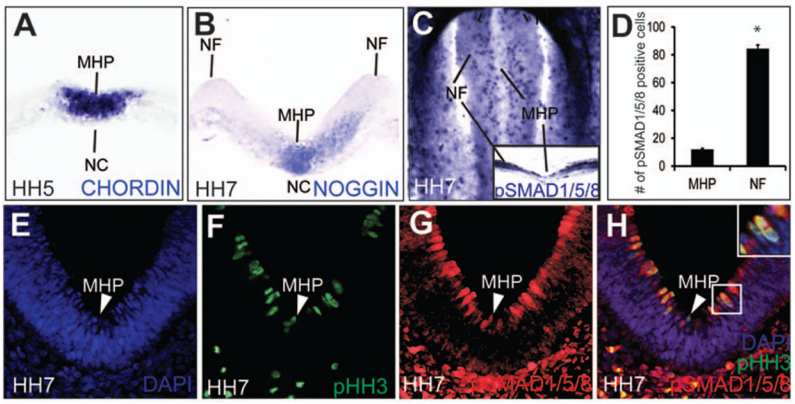

Figure 1. BMP signaling in the folding neural plate

(A) Chordin expression in the NC and the prospective MHP. **(B)** Noggin expression in the NC and the MHP. **(C–H) A 2-dimensional pSMAD 1,5,8 gradient in the neural plate.** (C, D) HH7 wholemount (top-down view, rostral to the top) showing a mosaic, latero-medial pSMAD 1,5, 8 gradient, with the low levels of pSMAD 1,5,8 at the MHP and higher levels in the neural folds (NF). Distribution of pSMAD 1,5,8+ cells along the lateral-medial axis is quantitated in D (# of lateral cells: 84.4; # of medial cells: 12; $p=3.84\times10^{-6}$.) (E-H). Cross-sectional views displaying latero-medially and apicobasally graded pSMAD 1,5, 8 expression (red) and its apical colocalization with mitotic (pHH3+, green) cells (arrowhead, E–H; boxed cell, H).

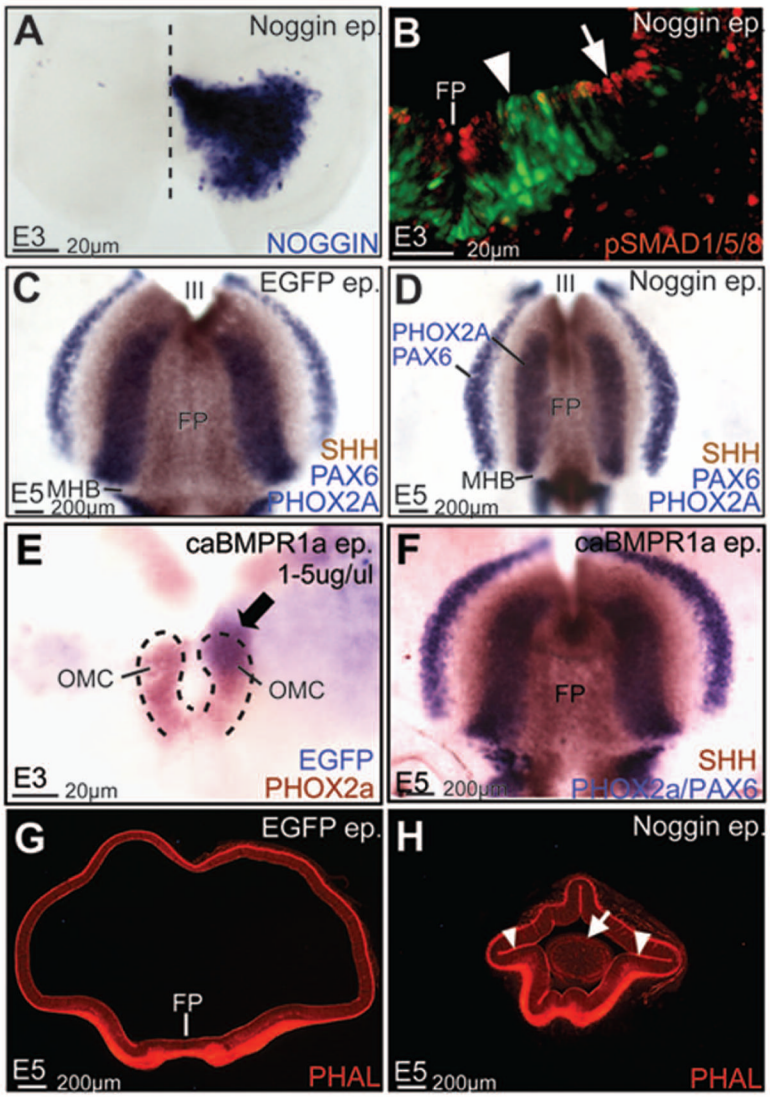

Figure 2. BMP signaling regulates midbrain shape, but not ventral cell-fate specification

(A) Unilateral Noggin misexpression in the midbrain (A, wholemount view, rostral to the top, ventricular surface facing the viewer). **(B)** Noggin (green) misexpression results in severely reduced pSMAD 1,5,8 (red) expression (compare arrowhead vs. arrow). **(C, D)** Control (C) and Noggin-electroporated midbrains (D, wholemount view, oriented as in A) demonstrating that ventral cell fates, assayed by *SHH* expression in the floor plate *(FP), PHOX2A* expression in oculomotor complex (OMC) neurons and *PAX6*, are not perturbed by BMP blockade. **(E, F)** Ventral midbrain cell fates (assayed as in C, D) are not affected by caBMPR1 electroporations at E3 or E5. Note that compared to C, the shape of the midbrain territories is altered in both D and E. Arrow in E points to caBMPR1 electroporation within the OMC territory. **(G, H)** Control (G) and Noggin-electroporations (H) demonstrating that Noggin induces ectopic hinge-like invaginations (arrowheads, H) and delaminated cells (arrow, H) in the lumen of the midbrain.

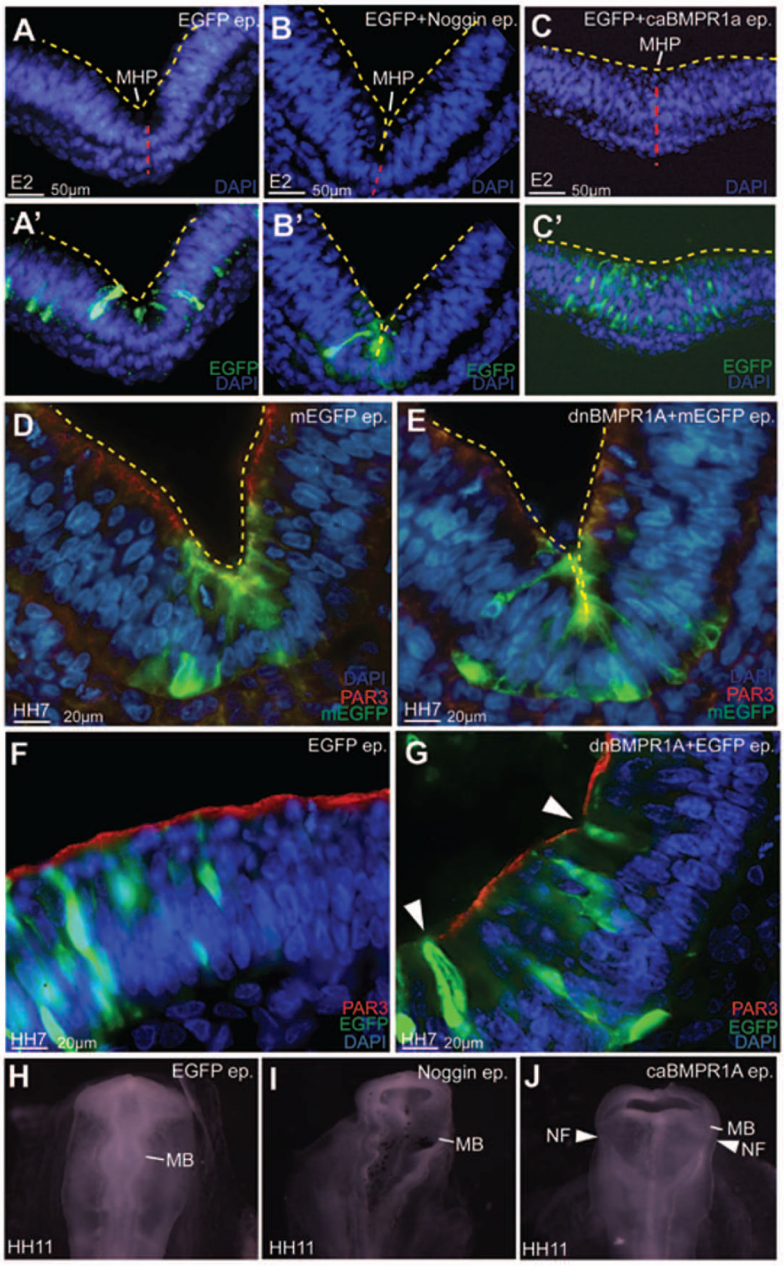

Figure 3. BMP blockade is necessary and sufficient for MHP formation

(A–C′) Bilateral electroporations of GFP (A, A′), Noggin-IRES-GFP (B, B′) and caBMPR1+GFP at HH7–9 demonstrating that compared to controls (A, A′), the MHP is exaggerated in Noggin-electroporated brains (B, B′) and flattened in caBMPR1-electroporated brains (C, C′). Red line marks the ventral midline. Yellow lines mark the apical/ventricular surface in A–E. **(D, E)** An exaggerated MHP following HH4–6 dnBMPR1a electroporations. Note that the effects of dnBMPR1 are non-autonomous. **(F, G)** Ectopic HPs induced in lateral neural plate following early dnBMPR1 manipulations (arrowhead in G). **(H–J)** HH11 embryos electroporated at HH4–6 showing normal neural tube closure in control (H), but not Noggin (I) or caBMPR1A (J) electroporated midbrains.

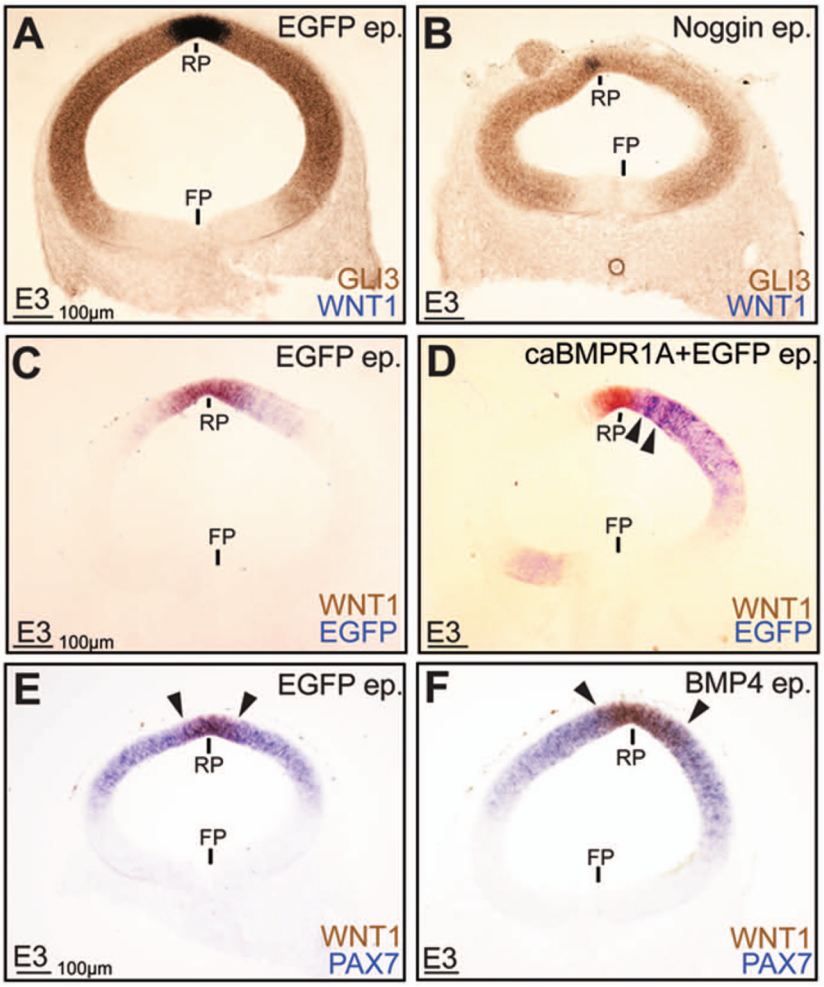

Figure 4. BMP signaling affects roof-plate specification, but not overall dorsal cell-fate specification

(A, B) Dorsal EGFP (A) and Noggin (B) electroporations demonstrating reduced *WNT1* expression in the Noggin-electroporated roof plate (RP), although the ventral limit of *GLI3* expression is unaltered. Note the presence of a cyst/rosette at the top left of Fig. 4B. **(C–F)** Dorsal EGFP (C) and caBMPR1 (D) electroporations demonstrating increased *WNT1* expression in D, F, while *PAX7* expression remains unaltered (E, F). Arrowheads in D mark the ectopic expression of *WNT1* outside the roof plate (RP), while arrowheads in E and F mark the lateral edges of the RP in control (E) and BMP4 (F) electroporated dorsal midbrains.

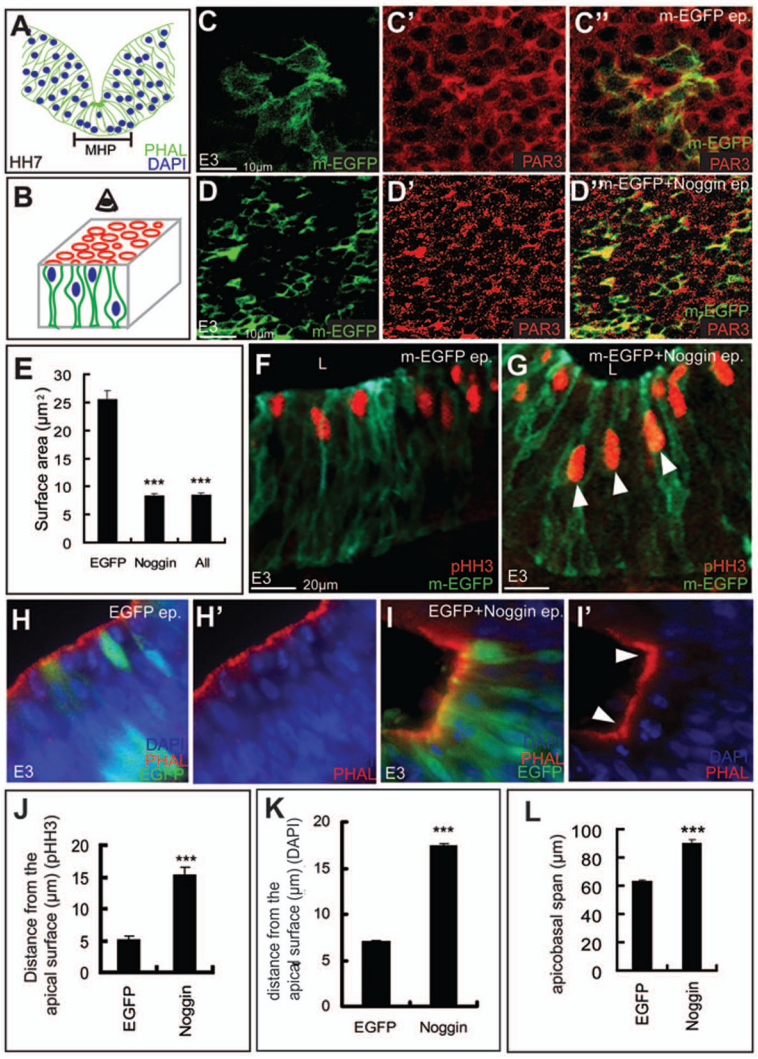

Figure 5. BMP signaling regulates apicobasal cell behaviors associated with MHP formation

(A) HH7 cartoon showing apically constricted cells with basally located nuclei (blue) at the MHP. **(B)** Cartoon depicting both the apical (red) surface and the apicobasal (green cells) axis of the neural tube. **(C–D″)** m-EGFP (green) electroporations displaying the apical surface areas (PAR3+, red) in control cells (C-C″). D, D″, strong, autonomous (green cells) and non-autonomous apical constriction is seen in Noggin-electroporated midbrains. **(E)** Quantitation of C–D″. Apical surface area: control cells: 25.79μm^2; Noggin-electroporated cells: 8.35μm^2; p=5.67×10^{-21}. **(F, G, J)** pHH3 immunostaining demonstrating aberrant, subapical (G, arrowheads) mitosis in Noggin-electroporated brains (G) compared to controls (F). (J) Quantitation of F, G. Distance from the apical surface, control: 5.2μm; Noggin: 15.32μm; p=2.32×10^{-19}. **(H–I′, K)** H, H′: EGFP electroporations displaying the smooth apical (PAR3+) contour of lateral midbrain and the normal distribution of DAPI-stained nuclei. I, I′: Noggin-induced ectopic hinge in lateral midbrain (arrowheads) displays apical constriction and basally located nuclei (I,I′). (K) Quantitation of overall basal nuclear migration. Distance from the apical surface: control cells: 8.15μm; n=56 cells/5brains; Noggin treated cells=18.14μm; n=78 cells/6 brains; p=3.15×10^{-7}. **(L)** Compared to controls, Noggin-electroporated cells display increased apicobasal spans. Apicobasal spans, EGFP-

electroporated cells: 49.2 μm, n=17 cells/5 brains, Noggin-electroporated cells: 72.52 um, 42 cells/10 brains; $p=1.05\times10^{-12}$. See also Fig. 6D, E.

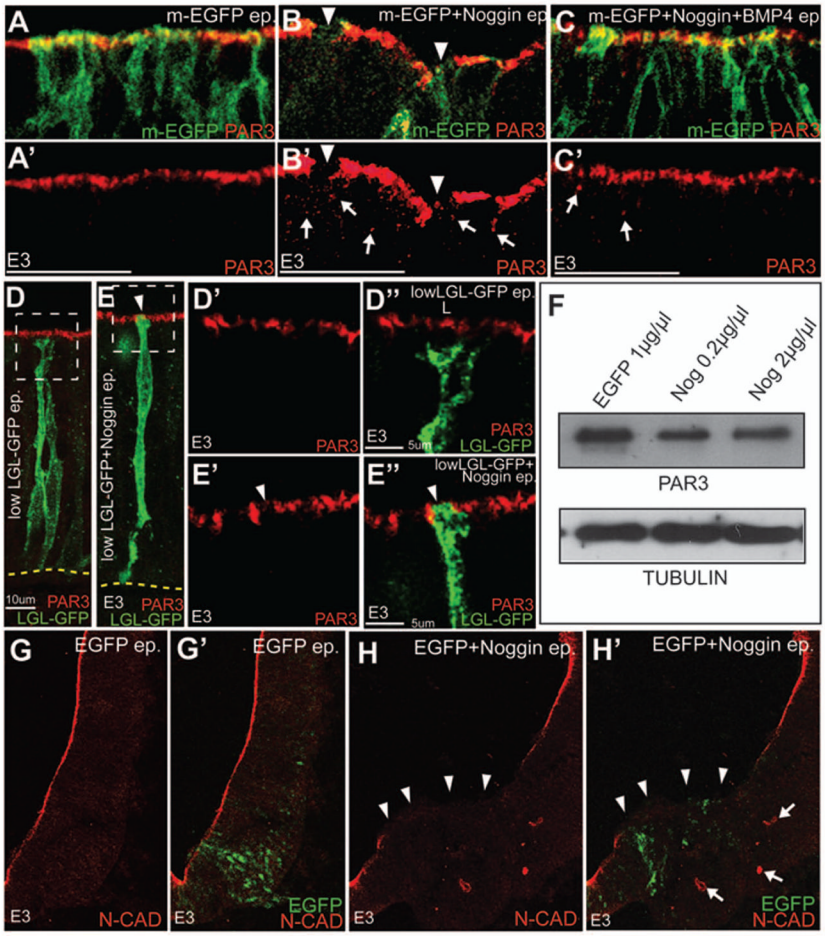

Figure 6. BMP signaling regulates epithelial apicobasal polarity

(A–C′) Confocal images showing that the downregulation of PAR3 (red, arrowheads B, B′) labeling from the apical surface of Noggin + m-EGFP (B, B′) electroporated cells can be partially rescued by co-electroporation of Noggin+BMP4 (C-C′). Control (m-EGFP only) electroporations are shown in A, A′. A′, B′ and C′ show the PAR3 channels for the merges shown in A, B and C respectively. **(D–E″)** Control LGL-GFP electroporations showing the segregation of the apical (PAR3+) and basolateral (LGL+) compartments (D-D″). Co-electroporation of Noggin with LGL-GFP (1µg/µl) results in the apical removal of PAR3 and the apical incursion of LGL-GFP (E-E″). **(F)** Western blots showing that PAR3 levels are not different between control and Noggin-electroporated E3 whole-cell lysates (*top row*). *Bottom Row*: loading controls. **(G–H′)** Confocal images demonstrating that reduced N-CAD expression at the apical membrane (arrowheads in H, H′) and the ectopic cytoplasmic expression of N-CAD (arrows in H, H′) in Noggin-electroporated brains (i, arrowheads). Controls shown in G, G′.

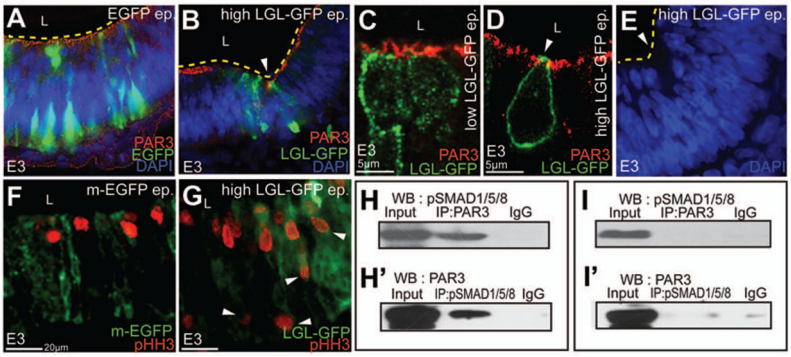

Figure 7. Perturbations of the apicobasal polarity pathway are sufficient to induce HP formation

(A–B) Unlike controls (A), high (5μg/μl) LGL-GFP misexpression is sufficient to induce ectopic HPs (arrowhead, B). (**C–D)** Control (C) and high LGL-GFP misexpression (D) demonstrating apical LGL, loss of apical PAR3 and apical constriction (arrowhead, D). **(E)** Compared to controls (A), nuclei are basally migrated at ectopic HPs induced by high LGL-GFP (E). **(F, G)** Aberrant, basal mitosis (arrowheads in G) following high LGL-GFP electroporations. (H–I′) Biochemical interactions between pSMAD 1,5,8 and PAR3 in EGFP-electroporated whole cell lysates immunoprecipitated with PAR3 and immunoblotted with pSMAD 1,5,8 antibody (H). pSMAD 1,5,8 and PAR3 interactions demonstrated by reversing pSMAD 1,5,8 and PAR3 antibodies (H′). Compared to controls (H, H′), biochemical interactions between pSMAD 1,5,8 and PAR3 are reduced in noggin-electroporated lysates (I, I′).

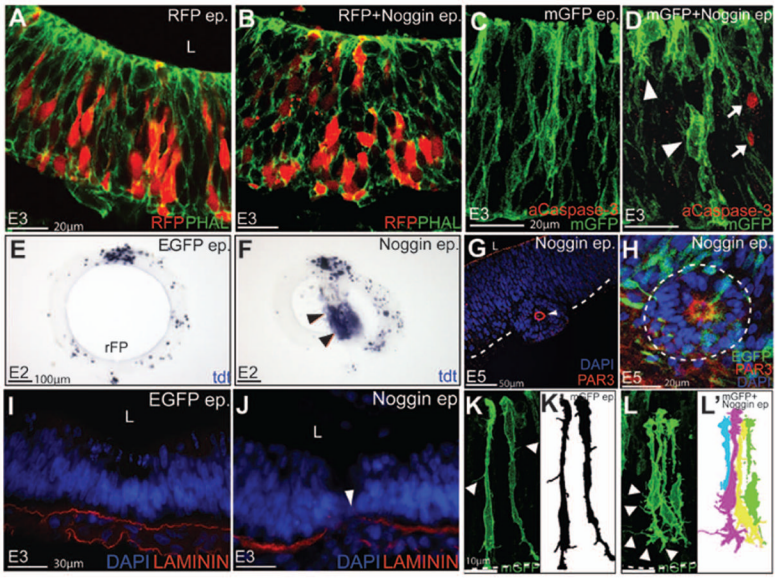

Figure 8. The epithelial dysmorphology resulting from BMP blockade is consistent with dysregulation of the apicobasal polarity pathway

(A, B) Compared to RFP-electroporated controls (A), non-autonomous disruption of epithelial organization (Phalloidin staining, green) is seen following Noggin +RFP electroporations (B). **(C, D)** Altered cell-shape changes (arrowheads D) can occur independently of the increased cell death (activated Caspase3+, arrows) seen in Noggin electroporated embryos. **(E, F)** Compared to controls (E), increased EMT and cell death are seen in the lumens of Noggin electroporated midbrains (arrowheads, F). **(G, H)** Cyst/rosette in Noggin-electroporated brains (arrowhead in G) display a re-organized polarity. Note that cyst has a defined (PAR3+) apical surface surrounding a DAPI-negative lumen (G). Note also that the majority of cells in the cyst are not electroporated (H). **(I, J)** EGFP and Noggin-electroporated midbrains displaying an intact (I) and a disrupted (arrowhead, J) Laminin+ basal lamina. **(K–L′)** EGFP electroporated midbrain progenitors displaying few filopodia-like-processes (arrowheads, K). Noggin electroporated cells displaying aberrant lateral filopodia (arrowheads, L). K′, L′ represent schematics of K and L respectively.

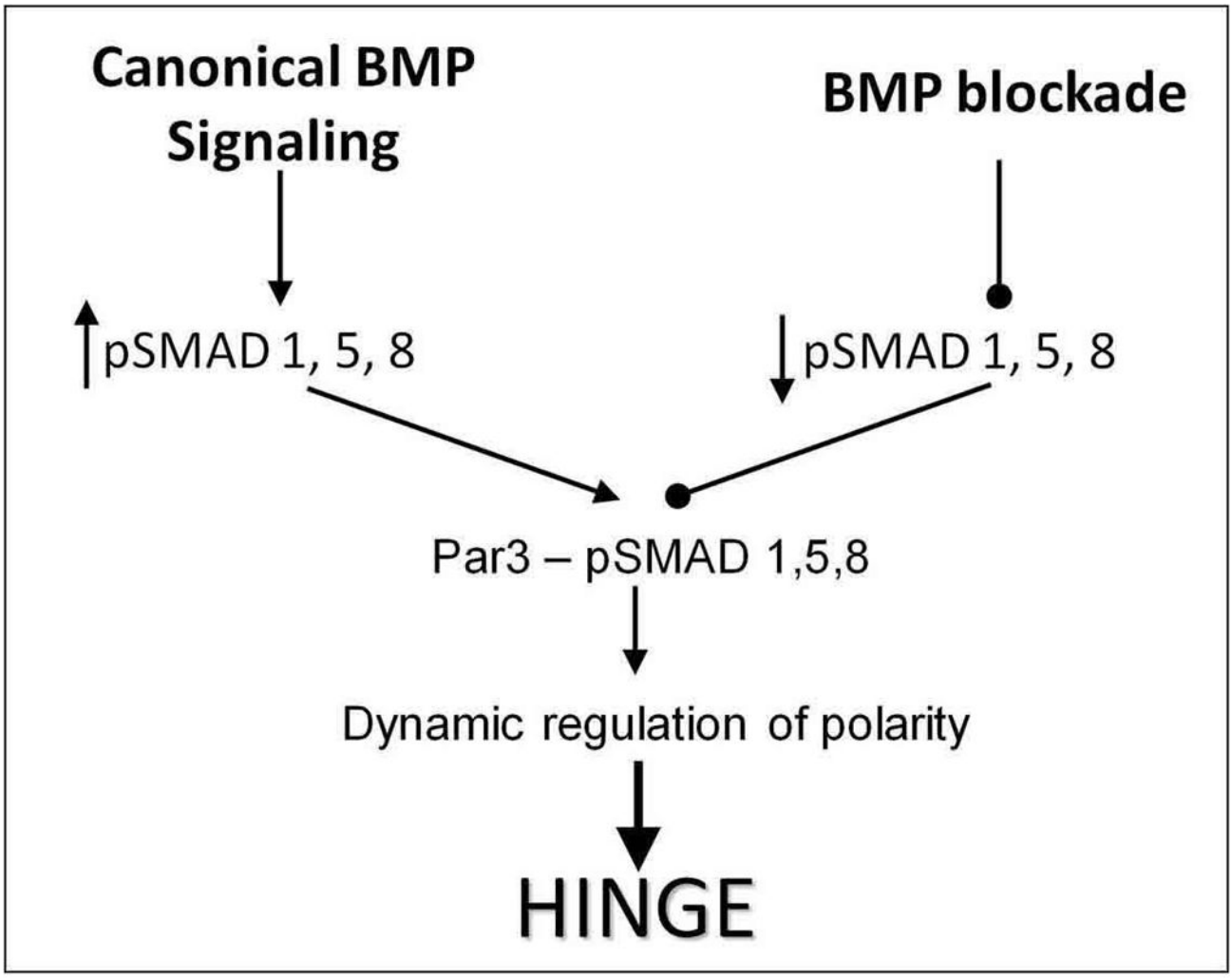

Figure 9. Summary depicting the role of BMP-polarity interactions in HP formation

Active BMP signaling induces SMAD1, 5, 8 phosphorylation, increasing pSMAD 1,5,8 interactions with the tight-junction associated PAR complex. These interactions stabilize the tight junction and thus neural epithelial organization. BMP blockade decreases the phosphorylation of SMAD1, 5, 8, reducing their interactions with the PAR complex. The partial loss of polarity modulates the junctional complexes sufficiently so that cells are more flexible and can undergo cell-shape changes required for HP formation and neural tube closure. Cyclic BMP signaling permits the dynamic modulation of polarity, but ensures that cells can change shapes without delaminating from the neural epithelium.